Science Signaling
AAAS
www.sciencesignaling.org/cgi/content/full/4/165/ra16/DC1

Supplementary Materials for

In Vivo Systems Analysis Identifies Spatial and Temporal Aspects of the Modulation of TNF-α–Induced Apoptosis and Proliferation by MAPKs

Ken S. Lau, Alwin M. Juchheim, Kimberly R. Cavaliere, Sarah R. Philips, Douglas A. Lauffenburger, Kevin M. Haigis*

*To whom correspondence should be addressed. E-mail: khaigis@partners.org

Published 22 March 2011, *Sci. Signal.* **4**, ra16 (2011)
DOI: 10.1126/scisignal.2001338

The PDF file includes:

Fig. S1. Basal proliferation and apoptosis in the small intestinal epithelium.
Fig. S2. Effects of loss of TNFR1 or TNFR2 on TNF-α–induced signaling.
Fig. S3. A representative TNF-α signaling network.
Fig. S4. Time courses of protein phosphorylation signals activated after intravenous administration of TNF-α in vivo.
Fig. S5. Total protein abundance and localization of activation in vivo.
Fig. S6. Statistical modeling of the TNF-α signaling network in vivo.
Fig. S7. Signaling data obtained after treatment with PD325901 or vehicle.
Fig. S8. Statistical modeling of TNF-α–induced apoptosis in the context of MEK inhibition.
Fig. S9. Statistical modeling of TNF-α–induced proliferation in the context of MEK inhibition.

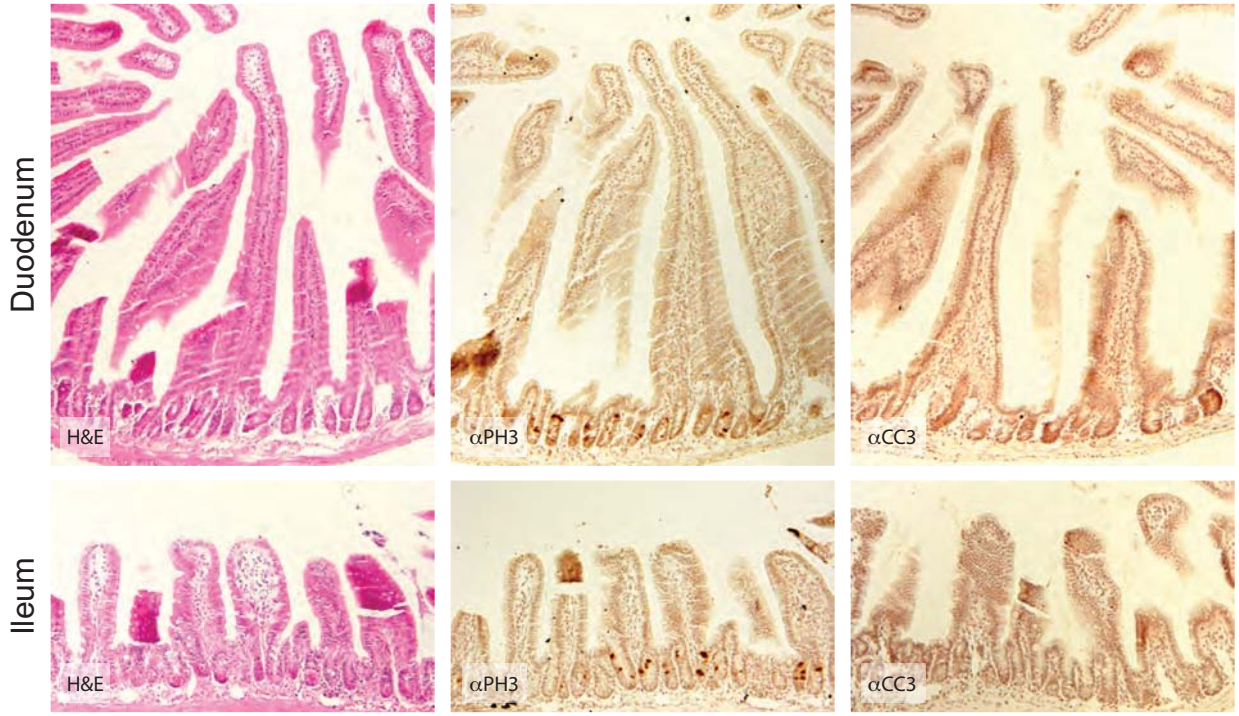

Fig. S1. Basal levels of proliferation and apoptosis in the small intestinal epithelium. The duodenum and ileum exhibit high basal rates of proliferation, as measured by immunohistochemical analysis of phosphorylated histone H3 (αPH3). By contrast, the basal levels of apoptosis are below the level of detection of cleaved caspase 3 by immunohistochemical analysis (αCC3).

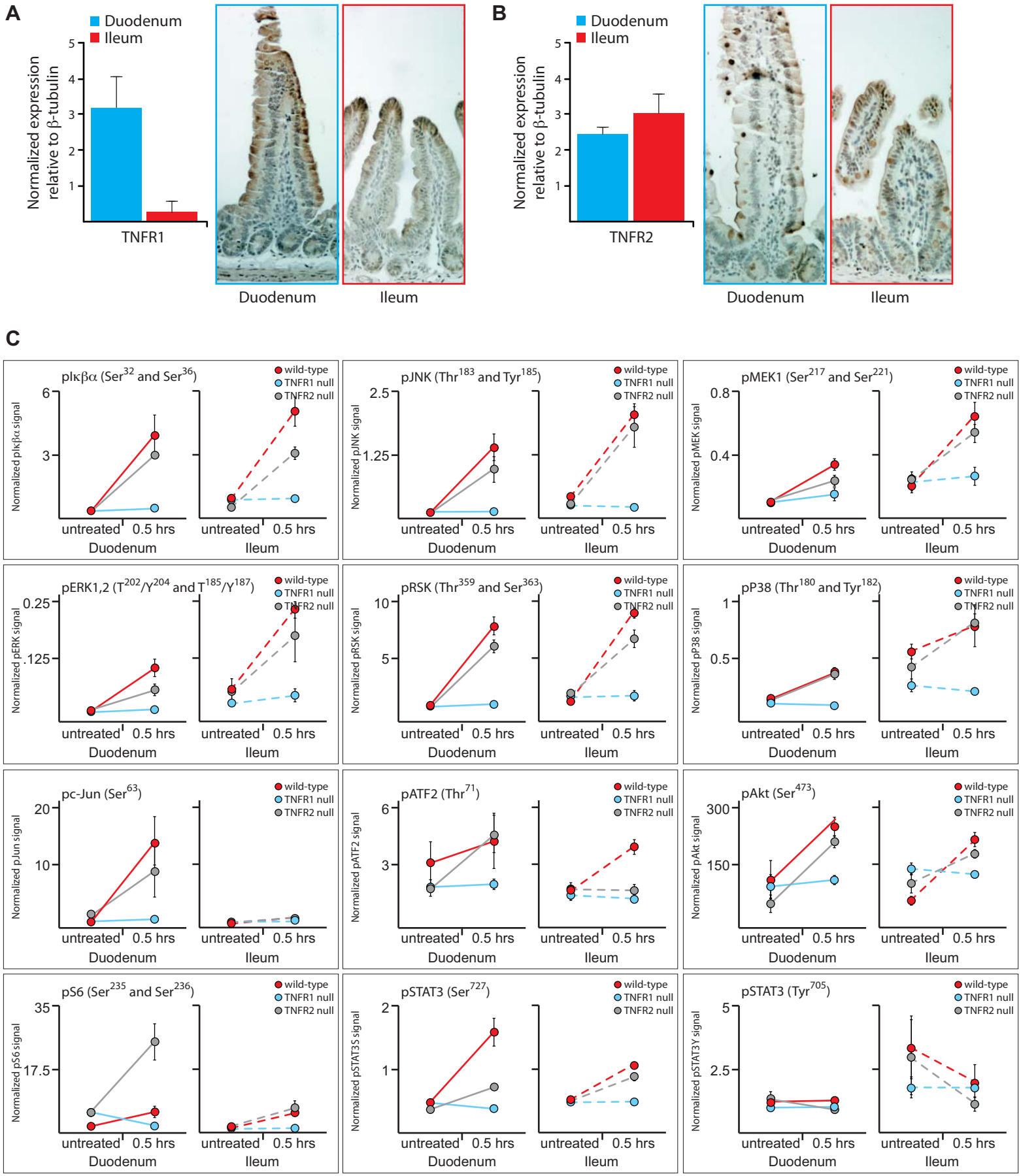
A
Duodenum
Ileum
Normalized expression relative to β-tubulin
TNFR1
Duodenum
Ileum
B
Duodenum
Ileum
Normalized expression relative to β-tubulin
TNFR2
Duodenum
Ileum
C
pIκβα (Ser32 and Ser36)
pJNK (Thr183 and Tyr185)
pMEK1 (Ser217 and Ser221)
pERK1,2 (T202/Y204 and T185/Y187)
pRSK (Thr359 and Ser363)
pP38 (Thr180 and Tyr182)
pc-Jun (Ser63)
pATF2 (Thr71)
pAkt (Ser473)
pS6 (Ser235 and Ser236)
pSTAT3 (Ser727)
pSTAT3 (Tyr705)
wild-type
TNFR1 null
TNFR2 null
untreated
0.5 hrs
Duodenum
Ileum

Fig. S2. Effects of loss of TNFR1 or TNFR2 on TNF-α-induced signaling. (**A**) Basal TNFR1 abundance in the duodenum and ileum of wild-type (WT) mice as determined by quantitative Western blotting and immunohistochemical analysis. Error bars represent the SEM from three independent experiments. (**B**) Basal TNFR2 abundance in the duodenum and ileum of WT mice as determined by quantitative Western blotting and immunohistochemical analysis. Error bars represent the SEM from three independent experiments. (**C**) Loss of TNFR1 completely abrogated signaling in response to TNF-α. Loss of TNFR2 partially abrogated signaling in response to TNF-α. Signaling data were obtained by Bio-Plex from control, untreated mice and from mice treated for 30 min with TNF-α (5 μg). Color schemes are based on genotype: red for WT, cyan for TNFR1-null, gray for TNFR2-null. Solid lines represent signaling data from duodenal samples, hashed lines represent signaling data from ileal samples. Error bars represent the SEM from four independent experiments.

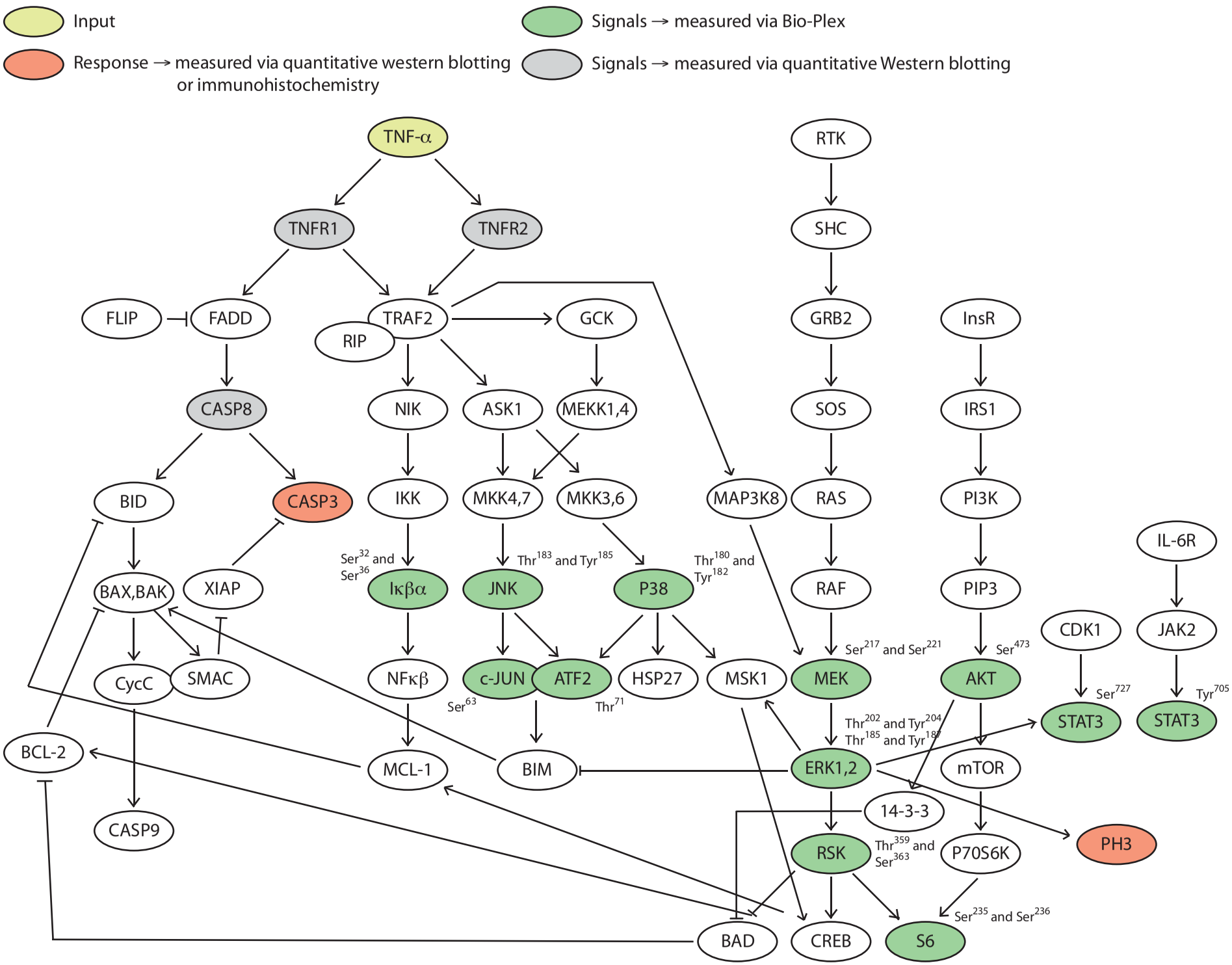
Input
Signals → measured via Bio-Plex
Response → measured via quantitative western blotting or immunohistochemistry
Signals → measured via quantitative Western blotting
TNF-α
TNFR1
TNFR2
FLIP
FADD
TRAF2
RIP
GCK
CASP8
NIK
ASK1
MEKK1,4
BID
CASP3
IKK
MKK4,7
MKK3,6
MAP3K8
BAX,BAK
XIAP
Ser32 and Ser36
IκBα
Thr183 and Tyr185
JNK
Thr180 and Tyr182
P38
CycC
SMAC
NFκβ
c-JUN
ATF2
HSP27
MSK1
Ser63
Thr71
BCL-2
MCL-1
BIM
CASP9
BAD
CREB
S6
RTK
SHC
GRB2
SOS
RAS
RAF
Ser217 and Ser221
MEK
Thr202 and Tyr204
Thr185 and Tyr187
ERK1,2
14-3-3
RSK
Thr359 and Ser363
Ser235 and Ser236
InsR
IRS1
PI3K
PIP3
Ser473
AKT
mTOR
P70S6K
PH3
IL-6R
JAK2
Tyr705
CDK1
Ser727
STAT3
STAT3

Fig. S3. A representative TNF-α signaling network. We aim to study how the cue (TNF-α, yellow) dynamically propagates information through the network to affect the phenotypic response (for example, apoptosis and proliferation as determined by detection of cleaved caspase 3 and phosphorylated histone H3, red). We sampled a wide range of signaling pathways by quantitatively measuring key protein phosphorylations with Bio-Plex signaling assays (green) or quantitative Western blotting (gray) over a time course after i.v. administration of TNF-α. Here, canonical pathways are depicted. Nevertheless, additional connections between the signaling molecules likely exist.

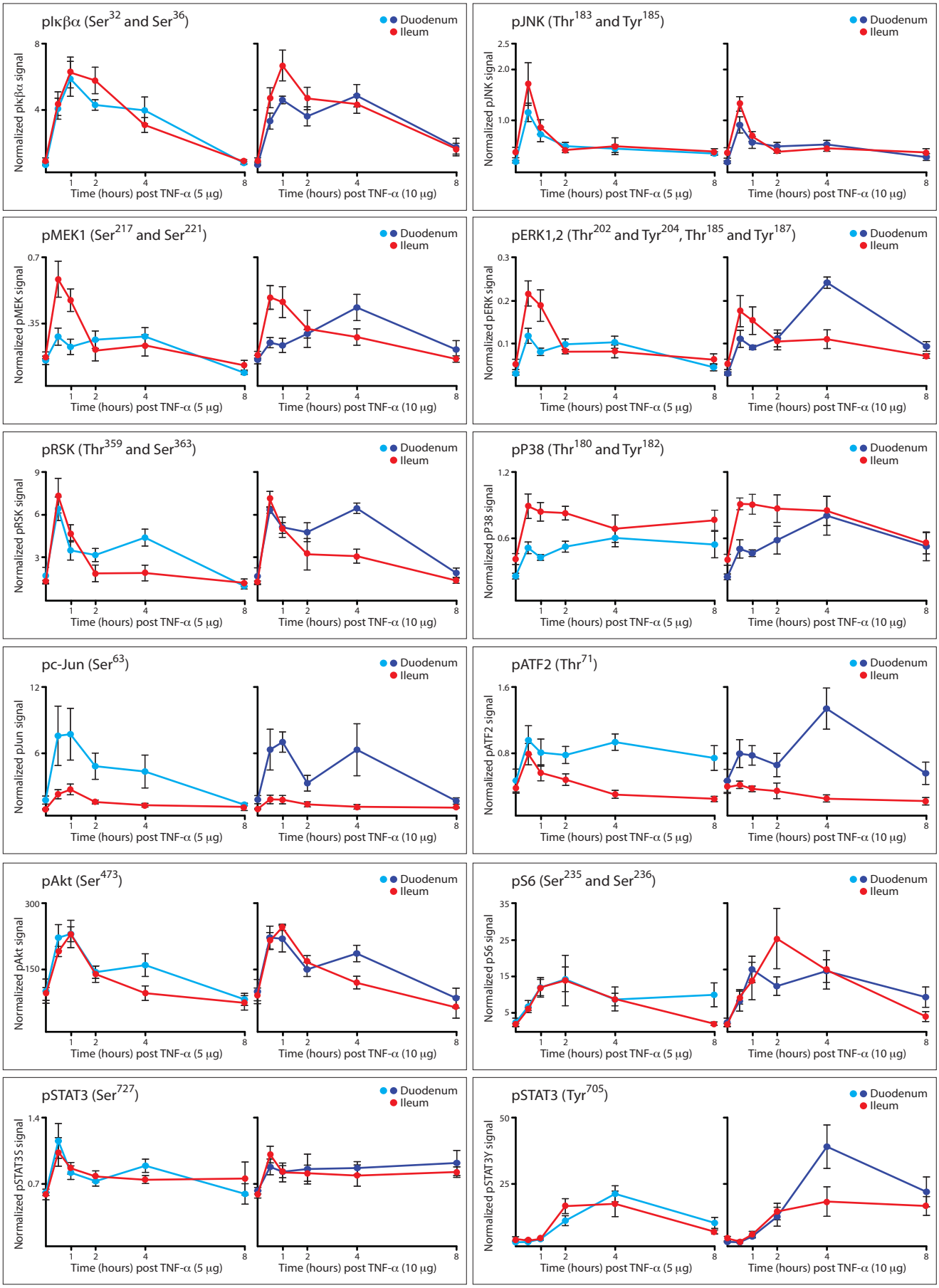
pIκβα (Ser32 and Ser36)
Duodenum
Ileum
Normalized pIκβα signal
Time (hours) post TNF-α (5 μg)
Time (hours) post TNF-α (10 μg)
pJNK (Thr183 and Tyr185)
Normalized pJNK signal
pMEK1 (Ser217 and Ser221)
Normalized pMEK signal
pERK1,2 (Thr202 and Tyr204, Thr185 and Tyr187)
Normalized pERK signal
pRSK (Thr359 and Ser363)
Normalized pRSK signal
pP38 (Thr180 and Tyr182)
Normalized pP38 signal
pc-Jun (Ser63)
Normalized pJun signal
pATF2 (Thr71)
Normalized pATF2 signal
pAkt (Ser473)
Normalized pAkt signal
pS6 (Ser235 and Ser236)
Normalized pS6 signal
pSTAT3 (Ser727)
Normalized pSTAT3S signal
pSTAT3 (Tyr705)
Normalized pSTAT3Y signal

Fig. S4. Time courses of protein phosphorylation signals activated after i.v. administration of TNF-α in vivo. Data points are the means of the median fluorescent intensities resulting from the phospho-protein assays, normalized between animals to a common positive control sample. Error bars represent the SEM from five independent experiments. Treatments with 5 and 10 μg of TNF-α are plotted on the same scale. Color schemes are based on region and dose: cyan for duodenum with 5 μg of TNF-α; blue for duodenum with 10 μg TNF-α; and red for ileum at either dose. Error bars represent the SEM from five independent experiments.

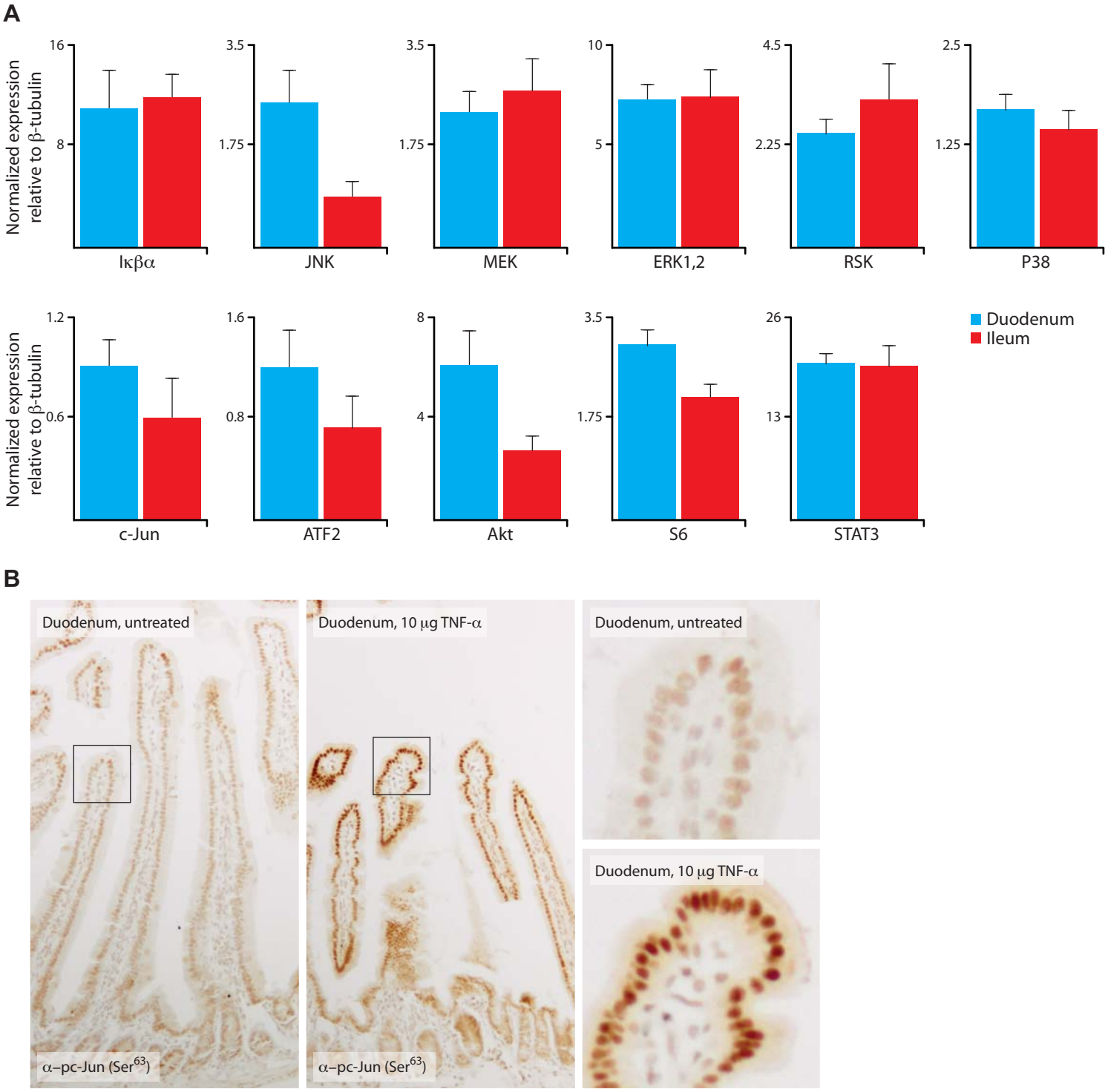

Fig. S5. Total protein abundance and localization of activation in vivo. (**A**) Total protein abundance in the duodenum (cyan) and ileum (red) in PBS-treated control mice, as assessed by quantitative Western blotting analysis. Data points are the means of the integrated fluorescent intensities of the bands, normalized to the intensity for β-tubulin in each sample. Error bars represent the SEM from three independent experiments. (**B**) Activation of c-Jun is localized to the intestinal epithelium. Immunohistochemical analysis of pc-Jun (Ser^{63}) demonstrated its localization to the intestinal epithelium of mice treated with TNF-α (10 μg) for 4 hours.

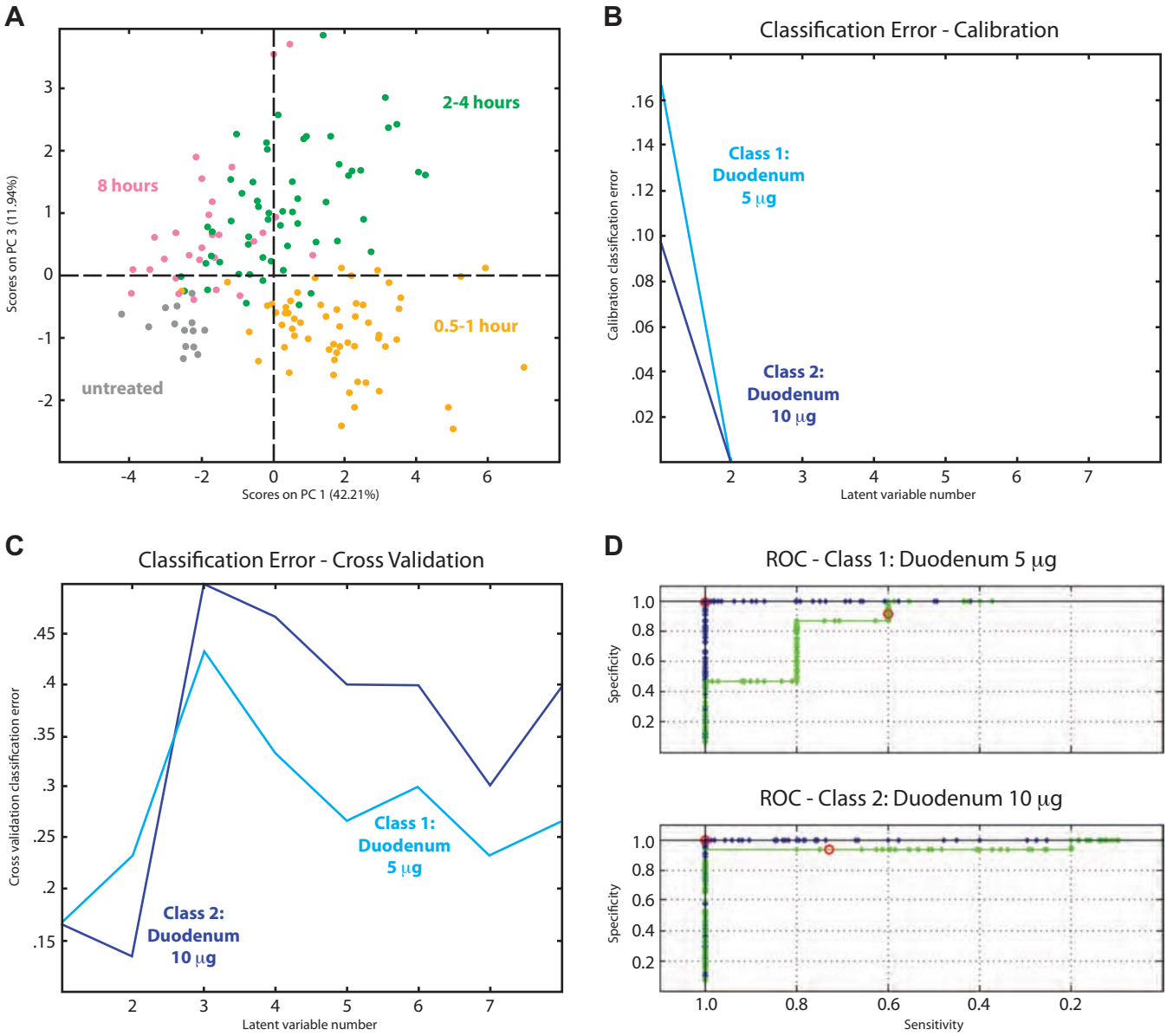
A
2-4 hours
8 hours
0.5-1 hour
untreated
Scores on PC 3 (11.94%)
Scores on PC 1 (42.21%)
B
Classification Error - Calibration
Class 1:
Duodenum
5 µg
Class 2:
Duodenum
10 µg
Calibration classification error
Latent variable number
C
Classification Error - Cross Validation
Class 1:
Duodenum
5 µg
Class 2:
Duodenum
10 µg
Cross validation classification error
Latent variable number
D
ROC - Class 1: Duodenum 5 µg
ROC - Class 2: Duodenum 10 µg
Specificity
Sensitivity

Fig. S6. Statistical modeling of the TNF-α signaling network in vivo. (**A**) A four-principal component PCA model captures time-course signaling information. PCA analysis was performed on the 12-dimensional signaling dataset with each sample arranged as a combination of time, mouse, and region. Scores generated by the model were plotted in principal component 1 and 3 space. Each score is colored by time. (**B**) A 2D PLSDA model describes dosage and regional effects on the TNF-α-induced apoptotic and proliferative phenotypes. Error of classification into class 1 (late apoptosis or arrest, cyan) and class 2 (early apoptosis or arrest, blue) of calibration data, using models with increasing numbers of latent variables. Classification error is defined as the probability of misclassifying a sample given the sample distribution and a model. (**C**) Error of classification into class 1 and class 2 of data kept out of the cross-validation procedure, using models built with the rest of the data, with increasing numbers of latent variables. (**D**) Receiver operating characteristic (ROC) curves depicting specificity (1-false positive rate) versus sensitivity (true positive rate) as the numerical threshold for classification is changed. The quality of a classification model can be evaluated by the degree by which the curves deviate from the center diagonal, with more deviation describing a better classification. ROC curves of class 1 and class 2 using a PLSDA with 2 LVs. The red circle represents the discriminant threshold selected for a model. The blue line represents the ROC curve for the model built with calibration data, and the green line represents the ROC curve for the model built with the cross-validation procedure.

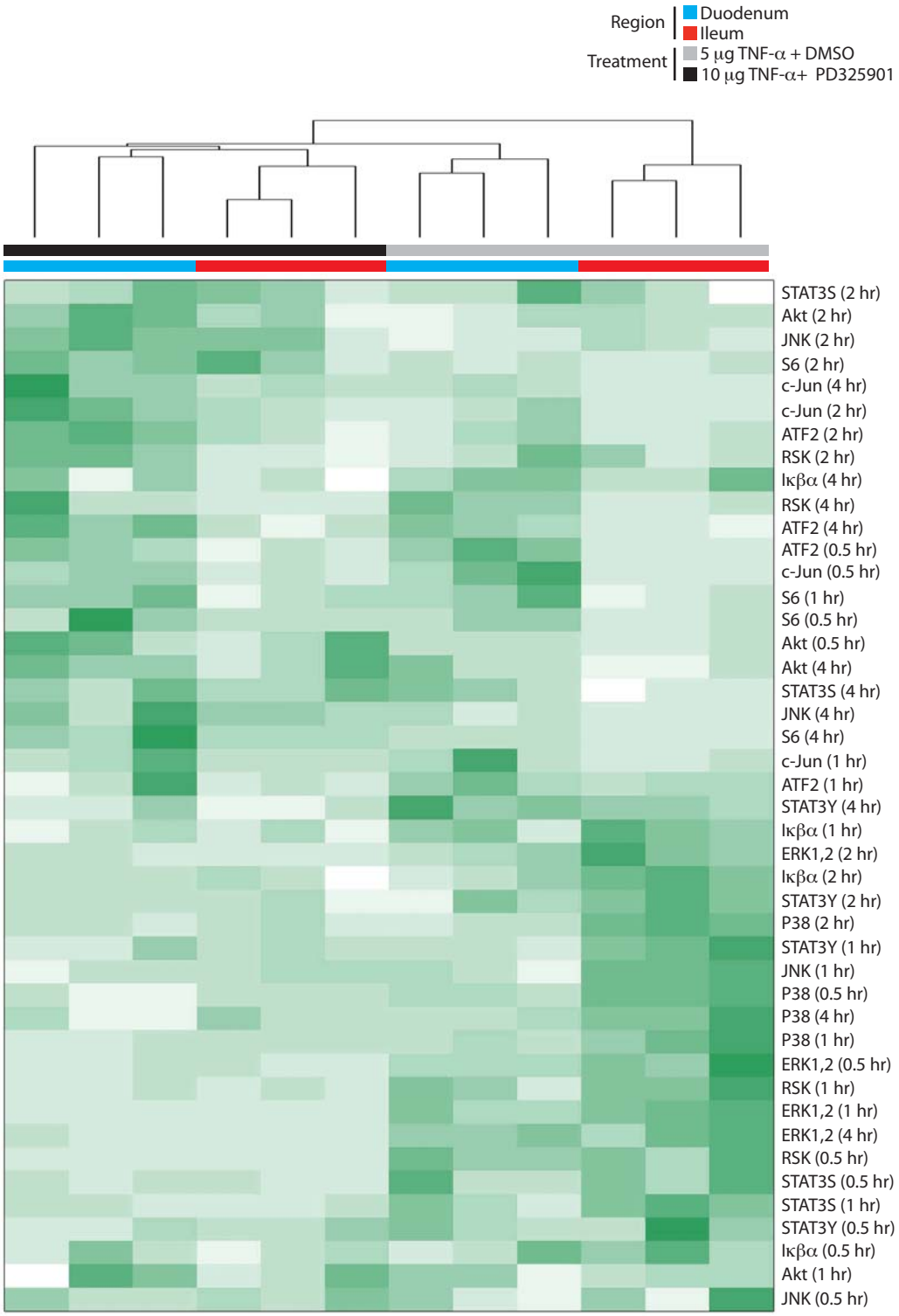

Fig. S7. Signaling data obtained after treatment with PD325901 or vehicle. Data were generated from the Bio-Plex signaling platform and are represented as a heat map of hierarchical clustering. The intensities of the green color represent the means of technical duplicates of the median fluorescent intensities (normalized to the highest value of each signal type here) resulting from each phospho-protein assay. Data are compiled from three independent experiments. Phosphorylated protein signals corresponding to each row are listed on the right side of the heat map.

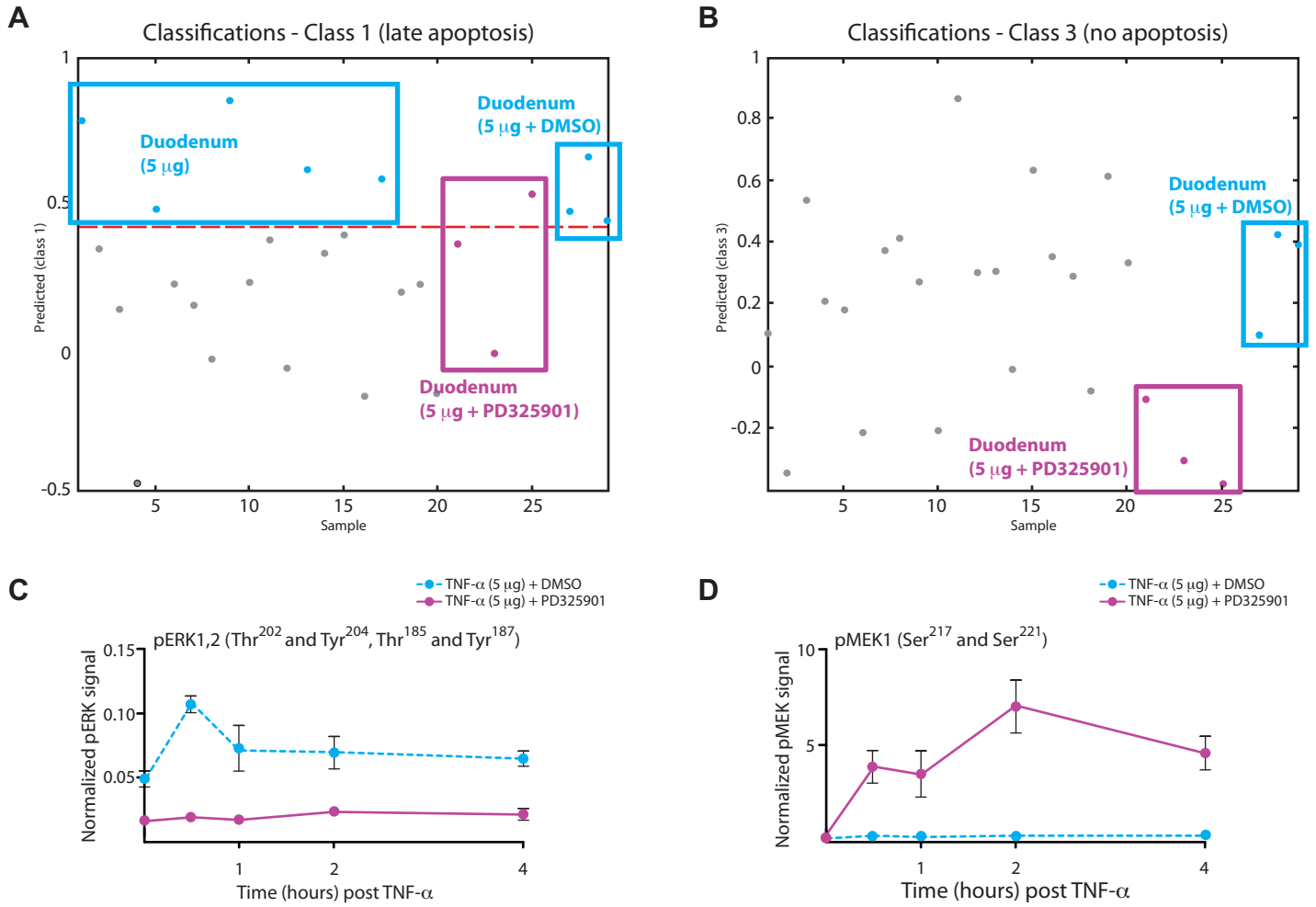

Fig. S8. Statistical modeling of TNF-α-induced apoptosis in the context of MEK inhibition. (**A**) A PLSDA model–based prediction of the apoptotic phenotype in the duodenum from phospho-protein signaling data from samples derived from animals treated with TNF-α after pre-treatment with PD325901 (purple) or DMSO vehicle control (cyan). The y-axis is the numerical result calculated with the PLSDA function of being classified into the "late apoptosis" (class 1) phenotypic class. The red broken line is the threshold that defines classification. (**B**) PLSDA model–based prediction of the classification into the "no apoptosis" (class 3) phenotypic class with signaling data of duodenal samples from animals treated with TNF-α after pre-treatment with PD325901 or DMSO. (**C**) Experimental amounts of pERK1,2 as determined by Bio-Plex in response to TNF-α (5 μg) after pre-treatment with PD325901 or DMSO. Error bars represent the SEM from three independent experiments. (**D**) Experimental amounts of pMEK as determined by Bio-Plex assay in response to TNF-α (5 μg) after pre-treatment with PD325901 or DMSO. Error bars represent the SEM from three independent experiments.

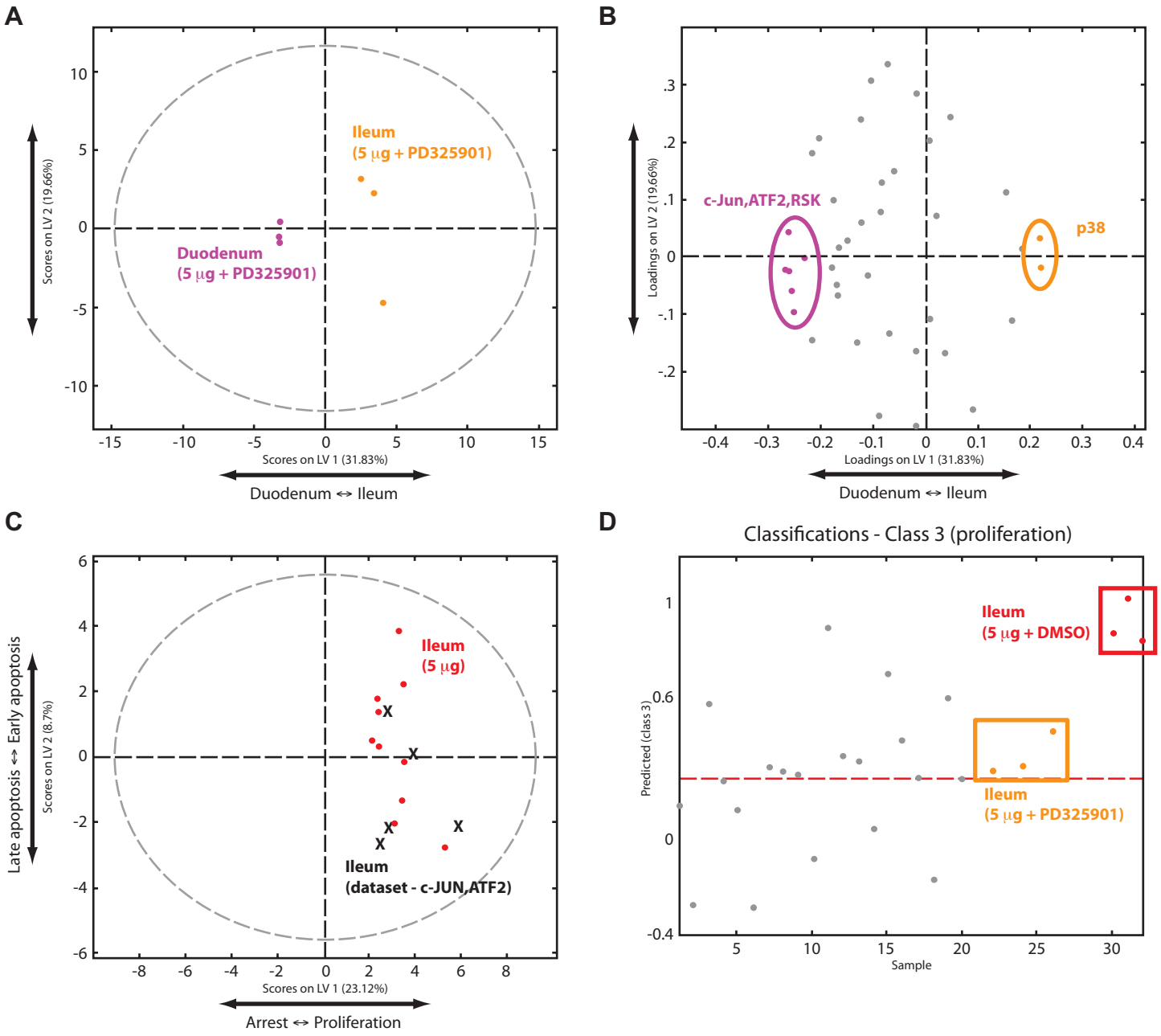

Fig. S9. Statistical modeling of TNF-α-induced proliferation in the context of MEK inhibition. (**A**) Scores of a 1D PLSDA model separating the duodenal from the ileal samples of animals treated with TNF-α and PD325901. Scores generated by the model plotted in 2 LV space (for visual purposes) are colored by region (ileum, orange; duodenum, purple). (**B**) Loadings generated by the model in (A) were plotted in 2 LV space. Loadings that clustered most with the PD325901-treated duodenal and ileal scores are colored and labeled. (**C**) Plot based on the PLSDA scores of an artificial dataset generated by excluding pc-Jun and pATF2 from the ileal samples (X) of the calibration dataset, relative to the ileal samples of the original calibration dataset (red). Note that the artificial dataset does not shift from the right side of the scores plot. (**D**) PLSDA model-based prediction of classification into the "proliferation" (class 3) phenotypic class with ileal signaling data from mice treated with TNF-α after pre-treatment with PD325901 (orange) or DMSO (red).